

**Measurement and modeling of the cross sections for the reaction  $^{230}\text{Th}(^3\text{He},3n)^{230}\text{U}$** A. Morgenstern,<sup>1,\*</sup> K. Abbas,<sup>2</sup> F. Simonelli,<sup>2</sup> R. Capote,<sup>3</sup> M. Sin,<sup>4</sup> B. Zielinska,<sup>1,†</sup> F. Bruchertseifer,<sup>1</sup> and C. Apostolidis<sup>1</sup><sup>1</sup>European Commission, Joint Research Centre, Institute for Transuranium Elements, P.O. Box 2340, 76125 Karlsruhe, Germany<sup>2</sup>European Commission, Joint Research Centre, Institute for Health and Consumer Protection, Cyclotron (TP-500), I-21020 Ispra (VA), Italy<sup>3</sup>NAPC-Nuclear Data Section, International Atomic Energy Agency, 1400 Vienna, Austria<sup>4</sup>Department of Nuclear Physics, University of Bucharest, P.O. Box MG-11, 70709 Bucharest-Magurele, Romania

(Received 28 March 2013; published 3 June 2013)

$^{230}\text{U}$  and its daughter nuclide  $^{226}\text{Th}$  are promising therapeutic nuclides for application in targeted  $\alpha$  therapy of cancer. We investigated the feasibility of producing  $^{230}\text{U}/^{226}\text{Th}$  via irradiation of  $^{230}\text{Th}$  with  $^3\text{He}$  particles according to the reaction  $^{230}\text{Th}(^3\text{He},3n)^{230}\text{U}$ . The experimental excitation function for this reaction is reported here. Cross sections were measured by using thin targets of  $^{230}\text{Th}$  prepared by electrodeposition, and  $^{230}\text{U}$  yields were analyzed by using  $\alpha$  spectrometry. Beam intensities were obtained via monitor reactions on aluminum foils by using high-resolution  $\gamma$  spectrometry and International Atomic Energy Agency recommended cross sections. Incident particle energies were calculated by using the SRIM-2003 code. The experimental cross sections for the reaction  $^{230}\text{Th}(^3\text{He},3n)^{230}\text{U}$  are in good agreement with model calculations by the EMPIRE-3 code once breakup and transfer reactions are properly considered in the incident channel. The obtained cross sections are too low to allow for the production of  $^{230}\text{U}/^{226}\text{Th}$  in clinically relevant levels.

DOI: [10.1103/PhysRevC.87.064602](https://doi.org/10.1103/PhysRevC.87.064602)

PACS number(s): 25.55.-e, 87.53.Jw, 24.10.-i, 27.90.+b

**I. INTRODUCTION**

The  $\alpha$  emitter  $^{230}\text{U}$  ( $T_{1/2} = 20.2$  d) and its daughter nuclide  $^{226}\text{Th}$  ( $T_{1/2} = 31$  min) are promising therapeutic nuclides for application in targeted  $\alpha$  therapy of cancer [1]. Both  $\alpha$  emitters decay through a rapid cascade of further  $\alpha$ -emitting daughter nuclides, generating a highly cytotoxic dose to targeted cancer cells. To facilitate their widespread medical application, the production of  $^{230}\text{U}/^{226}\text{Th}$  in clinically relevant amounts is a main prerequisite. In a series of investigations, we have studied three accelerator-driven processes for the production of  $^{230}\text{U}/^{226}\text{Th}$ , based on proton irradiation of  $^{232}\text{Th}$  and proton or deuteron irradiation of  $^{231}\text{Pa}$  [2–4]. These processes allow the production of the therapeutic nuclides in carrier-free form in clinically relevant levels.

Here, we report an alternative method for production of  $^{230}\text{U}/^{226}\text{Th}$ , based on the irradiation of  $^{230}\text{Th}$  with  $^3\text{He}$  ions. The target material  $^{230}\text{Th}$  is available from the decay chain of natural uranium. Our survey of literature data did not yield any relevant cross-sectional data on  $^3\text{He}$ -induced reactions on  $^{230}\text{Th}$ . Consequently, to investigate the productivity of the reaction  $^{230}\text{Th}(^3\text{He},3n)^{230}\text{U}$ , we have measured the excitation function of the reaction in the energy range of interest for production of  $^{230}\text{U}$ . In addition to its relevance for radionuclide production, the first measurement of the  $^{230}\text{Th}(^3\text{He},3n)$  reaction is also important as a benchmark of the modeling of  $^3\text{He}$ -induced nuclear reactions on heavy targets. Direct reactions are important in the incident channel for weakly bound projectiles (e.g., deuterons and  $^3\text{He}$ ) [5], but experimental data are needed to parametrize transfer and breakup reactions near and above

the Coulomb barrier. Additionally, fission is the dominant compound nucleus decay channel in studied reactions on actinides, therefore, a proper description of obtained experimental data is a consistency benchmark for fission-input parameters derived from the study of neutron-induced fission of corresponding  $^{233,232}\text{U}$  compound nuclei.

**II. EXPERIMENT****A. Sample preparation, irradiation conditions, and beam energy monitoring**

Solutions of nitric acid and hydrofluoric acid (HF) were prepared from suprapur grade reagents (Merck). Water was obtained from a Milli-Q water purification system. All other chemicals were reagent grade and were used as received.

$^{230}\text{Th}$  was purified from its daughter products by using extraction chromatography based on TEVA ion chromatography resin (50–100  $\mu\text{m}$ , Eichrom Technologies, LLC) as described in Ref. [6]. The resin was packed in a plastic column (Bio-Rad Laboratories, Inc.), which made up a bed volume of 0.5 ml. After conditioning the TEVA column with approximately 4-ml of 4M  $\text{HNO}_3$ , 0.5 ml of the sample solution that contained 1.8 mg of  $^{230}\text{Th}$  in 4M  $\text{HNO}_3$  was loaded onto the column. The column was washed with 9-ml 4M  $\text{HNO}_3$  to remove decay products, followed by elution of  $^{230}\text{Th}$  by using 0.02M  $\text{HNO}_3/0.02\text{M}$  HF solution. Approximately >97% of  $^{230}\text{Th}$  was recovered in a 2-ml eluate. The eluate was used directly for preparation of Th targets by electrodeposition based on the method described by Talvitie [7]. For electrolytic deposition of  $^{230}\text{Th}$ , 8.9 ml of 1M ammonium sulfate, adjusted to pH 2, was transferred to an electrolysis cell made from Plexiglas and 15  $\mu\text{l}$  of 0.02M  $\text{HNO}_3/0.02\text{M}$  HF solution, containing 8–15- $\mu\text{g}$   $^{230}\text{Th}$ , and 10  $\mu\text{l}$  of concentrated hydrofluoric acid were added to the cell. Silver plates of 99.99% purity with 0.1-mm thickness and 16-mm diameter were used as cathode materials, and a platinum wire was used as an

\*Corresponding author: [alfred.morgenstern@ec.europa.eu](mailto:alfred.morgenstern@ec.europa.eu)

†Present address: Department of Radiochemistry, Institute of Nuclear Chemistry and Technology, Dorodna 16, 03-195 Warsaw, Poland.

anode. Electrodeposition was carried out at a current of 1 A (voltage varied from 9.3 to 11 V) for 3 h. Five minutes before switching off the current, 1 ml of 10M sodium hydroxide was added. The cell was dismantled, and then, the silver disk was rinsed with water and ethanol and was dried by warming on a hot plate. Under these conditions,  $^{230}\text{Th}$  deposition rates that exceeded 99.9% were obtained. During electrodeposition, a hole mask of 9-mm diameter was used to obtain thorium layers of defined geometry containing 8.5–14.6  $\mu\text{g}$  of  $^{230}\text{Th}$ . The homogeneity of the  $^{230}\text{Th}$  layers was assessed by autoradiography (molecular imager FX, Bio-Rad Laboratories, Inc.) and was analyzed by using the QUANTITY ONE software (Bio-Rad Laboratories, Inc.). Targets were used for cross-sectional measurements if maximum variations in the thickness of the  $^{230}\text{Th}$  layers across the circular area were found to be less than 10%. Subsequently, the silver disks were covered with aluminum foils (22.5- $\mu\text{m}$  thickness, 99.99%, Alfa Aesar), which acted as catcher foils to avoid any losses of activity by recoil processes.

Irradiations were performed at the cyclotron of the Institute for Health and Consumer Protection of the European Commission, Joint Research Centre in Ispra, Italy.  $^3\text{He}$  irradiations of thin  $^{230}\text{Th}$  targets were performed at incident energies of 10.1–35.3 MeV by using currents of 0.94–2.4  $\mu\text{A}$  for 254–420 min. During irradiations, a beam collimator of 7-mm diameter was used to focus the beam on the thorium layer of 9-mm diameter, and the backside of the targets was cooled with water. Aluminum foils of 22.5- $\mu\text{m}$  thickness (99.99%, Alfa Aesar), used as monitor foils, were placed in front of the targets during irradiation.

Beam energies extracted from the cyclotron were determined from the beam-orbit position measurements. The energies that entered the thorium target layers were calculated by using the SRIM-2003 code [8], which took into account the loss of  $^3\text{He}$  particle energy in the cover and monitor foils. Beam intensities were determined based on the  $^{27}\text{Al}(^3\text{He},x)^{22}\text{Na}$  monitor reaction by using International Atomic Energy Agency (IAEA) updated recommended cross-sectional data [9]. Decay data for  $^{22}\text{Na}$  were taken from Ref. [10].

## B. Measurement of radioactivity

High-resolution  $\gamma$  spectrometry of activated monitor foils was performed by using a high-purity germanium detector system. To increase accuracy and precision of the activity measurements, several HPGe detectors, calibrated in energy and efficiency in different geometries by using certified standard radioactive sources (National Agency for New Technologies, Energy and Sustainable Economic Development (ENEA), Italy and Commissariat à l'énergie atomique et aux énergies alternatives, Département des Applications et de la Métrologie des Rayonnements Ionisants (CEA-DAMRI) and Compagnie pour l'Etude et la Réalisation de Combustibles Atomiques (CERCA), France), were used to acquire different  $\gamma$ -ray spectra for each of the activated foils. Two  $\gamma$ -ray spectrum analysis software packages were used, the GAMMA VISION acquisition system (Model A66-B32, Version 5.10, EG&G ORTEC, USA) and GENIE 2000 (CANBERRA Industries, Inc., USA). The activity measurement of  $^{230}\text{Th}$  and  $^{230}\text{U}$

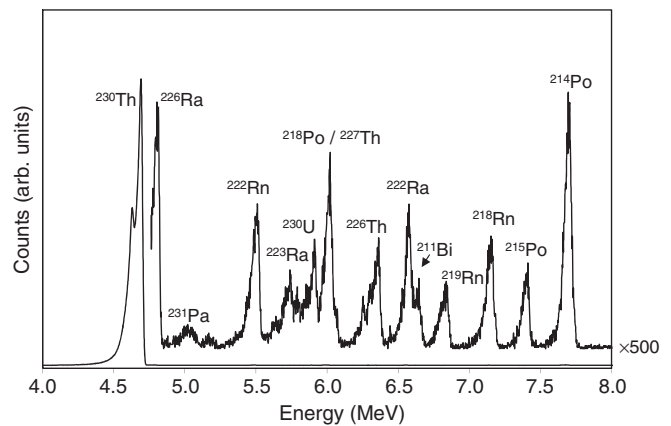


FIG. 1.  $\alpha$  spectrum of  $^{230}\text{Th}$  after irradiation with  $^3\text{He}$  particles at 29 MeV. The inset is magnified 500 times.

in individual thin foils was performed by  $\alpha$  spectrometry (Soloist, EG&G ORTEC). The efficiency of the  $\alpha$  detector was calibrated by using a mixed  $^{239}\text{Pu}/^{241}\text{Am}/^{244}\text{Cm}$  standard (AMR43, Amersham). Counting times varied from 30 to 4210 min, which depended on sample activity.

Aluminum cover foils were removed from the silver target foils that contained the  $^{230}\text{Th}/^{230}\text{U}$  layer, and both foils were measured by  $\alpha$  spectrometry. The direct  $\alpha$  spectrometric measurement of the activated silver target foils resulted in  $\alpha$  spectra of low resolution and did not allow the determination of the activities of  $^{230}\text{Th}$  and  $^{230}\text{U}$  due to spectral interferences. Consequently, the activated layers were dissolved by stepwise addition of  $2 \times 50 \mu\text{l}$  of 6M hydrochloric acid with a yield that ranged from 74% to 100%. An aliquot of the resulting solution was added onto a new silver disk to prepare samples for  $\alpha$  spectrometry by evaporation. The residual silver target foils were dried and were counted by  $\alpha$  spectrometry. This procedure led to  $\alpha$  spectra of high resolution as illustrated in Fig. 1, which shows typical  $\alpha$  spectra obtained from a  $^{230}\text{Th}$  target irradiated with  $^3\text{He}$  particles of 29-MeV energy. Decay data for the  $\alpha$  emissions of  $^{230}\text{Th}$  and its daughter nuclides are taken from Ref. [11], and decay data for  $^{230}\text{U}$  and its daughter nuclides are taken from recent measurements [12–15] (Table I). Analysis of the  $\alpha$  spectra revealed spectral interferences between the  $\alpha$  emissions of  $^{230}\text{U}$  ( $E_\alpha = 5.818$  and 5.888 MeV) and  $^{218}\text{Po}$  ( $E_\alpha = 6.003$  MeV) generated through the decay of  $^{230}\text{Th}$  as well as with  $^{223}\text{Ra}$  ( $E_\alpha = 5.607$  and 5.716 MeV) generated from the decay of low levels of  $^{231}\text{Pa}$  impurities contained in the  $^{230}\text{Th}$  starting material. Therefore, the activity of  $^{230}\text{U}$  was determined *via* analysis of the  $\alpha$  emission of its daughter nuclide  $^{218}\text{Rn}$  at 7.129 MeV after radioactive equilibrium was reached.

## C. Determination of cross sections and uncertainties

Cross sections were calculated by using the activation equation based on beam current, target thickness, and reaction product activity. There are several major contributions to the overall uncertainty of the determined cross sections. The uncertainty of the beam current measurement, which is given by the uncertainty of the published cross sections used for the calculation of the beam current (<10%), the uncertainty in the

TABLE I. Principal  $\alpha$  emissions (emission probability  $>0.1$ ) of  $^{230}\text{Th}$ ,  $^{230}\text{U}$ , and their  $\alpha$ -particle-emitting daughter nuclides [11–15].

Nuclide	Half-life	Energy (MeV)	Emission probability	Nuclide	Half-life	Energy (MeV)	Emission probability
$^{230}\text{Th}$	$7.54 \times 10^4$ years	4.688	0.763	$^{230}\text{U}$	20.2 d	5.888	0.674
		4.621	0.234			5.818	0.320
$^{226}\text{Ra}$	$1.60 \times 10^3$ years	4.784	0.940	$^{226}\text{Th}$	30.7 min	6.337	0.754
		4.601	0.060			6.234	0.229
$^{222}\text{Rn}$	3.82 d	5.490	0.999	$^{222}\text{Ra}$	33.6 s	6.559	0.969
$^{218}\text{Po}$	3.10 min	6.003	1.000	$^{218}\text{Rn}$	33.8 ms	7.129	0.999
$^{214}\text{Po}$	$164 \mu\text{s}$	7.687	1.000	$^{214}\text{Po}$	$164 \mu\text{s}$	7.687	1.000
$^{210}\text{Po}$	138 d	5.304	1.000				

thickness of the monitoring foil ( $<2\%$ ), and the uncertainty in the determination of the activity of  $^{22}\text{Na}$ , include the uncertainty of its decay data ( $<5\%$ ). Furthermore, the uncertainty in the thickness of the irradiated  $^{230}\text{Th}$  layer ( $<10\%$ ) and in the determination of  $^{230}\text{U}$  activity ( $<5\%$ ) is included. The uncertainty associated with dissolution of the  $^{230}\text{Th}$  target layer and preparation of new samples for  $\alpha$  spectrometric measurements is mainly related to the measurement of the volume of the resulting solution ( $<2\%$ ) and possible losses of activity during sample evaporation, which are considered to be negligible. The overall uncertainty in the determination of the  $^{230}\text{U}$  cross sections was, thus,  $<16.1\%$ . The uncertainty of the beam energy determined from the beam-orbit position measurements corresponds to 0.2 MeV.

### III. NUCLEAR-REACTION MODELING

Cross sections of the reactions, induced by  $^3\text{He}$  projectiles on  $^{230}\text{Th}$  targets in the energy range of 10–35 MeV, have been calculated with the modular system EMPIRE-3.1 RIVOLI [16–18], which uses updated nuclear-reaction models to describe the direct, preequilibrium, and compound nucleus emission mechanisms relevant to the studied energy range. The optical model calculations of the direct cross sections and particle transmission coefficients were performed with the ECIS06 code [19] incorporated into the EMPIRE-3.1 system. Breakup and transfer reaction cross sections were calculated by using the phenomenological models given by Kalbach Walker in Refs. [20,21]. Preequilibrium emission was taken into account by the module PCROSS featuring a one-component exciton model with  $\gamma$ , nucleon, and cluster emissions. The compound nucleus mechanism was described by the Hauser-Feshbach statistical model, which includes decay probabilities deduced in the optical model for fission [22–24] and accounts for the multiple-particle emission and the full  $\gamma$  cascade.

We have reported similar calculations for alternative production routes of  $^{230}\text{U}/^{226}\text{Th}$  based on proton or deuteron irradiation [2–4]. However, we faced new challenges in this investigation mainly related to the required treatment of the direct interaction mechanism in the incident channel. First, we notice the absence in the Reference Input Parameter Library (RIPL)-3 database [25] of an optical model potential (OMP) that describes the interaction of  $^3\text{He}$  projectiles with a  $^{230}\text{Th}$  target nucleus. Therefore, we selected the OMP RIPL8100 [26] derived for  $^3\text{He}$  projectile energies up to 40 MeV incident on

targets with  $Z \leq 82$ . The prediction power of this OMP and of the other theoretical models involved was initially tested on  $^{197}\text{Au}$ ,  $^{208}\text{Pb}$ , and  $^{209}\text{Bi}$  nuclei. The advantages of using these lighter target nuclei are as follows: (i) fission contribution to the reaction cross section is very small up to 40 MeV of incident energy, so there is no uncertainty associated with fission barrier parameters; (ii)  $2n$ ,  $3n$ , and  $4n$  outgoing reaction channels are dominant in their corresponding energy ranges; (iii) experimental data for ( $^3\text{He},2n$ ), ( $^3\text{He},3n$ ), and ( $^3\text{He},4n$ ) reactions are often available. Our calculated neutron-emission cross sections overestimated the experimental data especially below the Coulomb barrier. Such an overestimation was expected as direct reaction processes are known to play a significant role in the description of complex-projectile-induced reactions near the Coulomb barrier as already observed for deuteron-induced reactions in Ref. [5]. By including breakup and transfer reactions in the incident channel, we achieved a reasonably good description of all available experimental data. It should be noted that the direct reaction parametrization of Kalbach Walker [20,21] was modified below the Coulomb barrier to make it compatible with the OMP-calculated direct reaction cross section. The original parametrization was multiplied by the following barrier penetrability factor:

$$f(E) = \frac{1}{1 + \exp\left(\frac{V-E}{D}\right)},$$

where  $V$  and  $D$  are parameters that define the barrier properties and  $E$  is the  $^3\text{He}$  projectile energy. We used the following parameter values:  $D = 1.6$  and  $V = 22$  MeV. This modification amounts to a proper consideration of the Coulomb barrier penetrability in Kalbach Walker's parametrization as found for deuteron projectiles by Avrigeanu *et al.* [5].

Once the OMP RIPL8100 was selected and was tested, we assumed its validity for the case of  $^3\text{He}$ -induced reactions on  $^{230}\text{Th}$ . The particle transmission coefficients for the emerging nucleon channels were calculated by using the dispersive nucleon potential developed for actinides (RIPL 2408/5408 for neutrons and protons, respectively [27,28]). The nuclear-level densities calculated in the previous studies [2–4] with the enhanced generalized superfluid model (EGSM) [17] have been replaced with semimicroscopic combinatorial-level densities (the Hartree-Fock-Bogoliubov method) [25], [29] mainly because of the uncertainty in the EGSM related to the poorly known discrete-level schemes of  $^{230,231}\text{U}$  nuclei. The

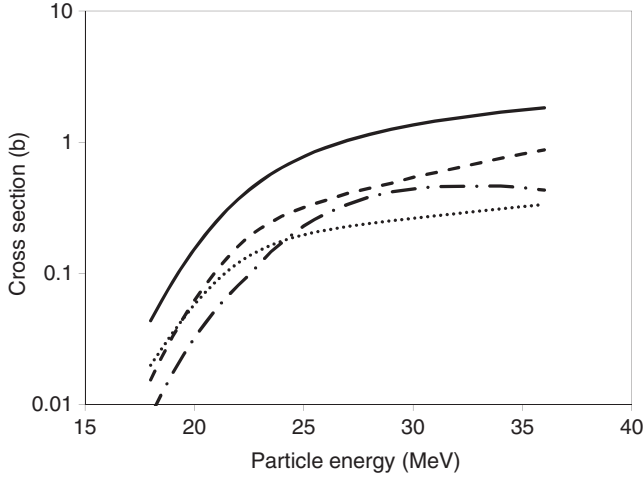


FIG. 2. Model calculations for the reaction  ${}^3\text{He} + {}^{230}\text{Th}$  that shows the contribution to the reaction cross section of different reaction mechanisms and the fission channel (solid line: reaction; dotted line: breakup; dashed line: transfer; and dashed-dotted line: fission).

fission barrier parameters used in the calculations have been derived from the analysis of neutron-induced fission reactions  ${}^{232}\text{U}(n,f)$  and  ${}^{233}\text{U}(n,f)$  and have been slightly adjusted within uncertainty limits. The level densities at the saddles were calculated by using the EGSM but with parameters and enhancement factors specific to the corresponding deformations of the nuclear shape. It should be mentioned that the fission parameters used in the present calculations were very close (and consistent within the estimated uncertainty) to those used for the emissive fission chances in the previous studies [2–4]. Additional required input parameters were retrieved from the RIPL-3 database [25].

By using the nuclear models and parameters described above, the calculations of all possible reactions have been undertaken for  ${}^3\text{He}$ -induced reactions on  ${}^{230}\text{Th}$  up to 36-MeV  ${}^3\text{He}$  incident energy. Further studies are necessary to find general prescriptions to estimate breakup and transfer cross

TABLE II. Experimental cross sections for the reaction  ${}^{230}\text{Th}({}^3\text{He},3n){}^{230}\text{U}$ .

Energy (MeV)	Cross section (mb)
$10.1 \pm 0.2$	0
$18.7 \pm 0.2$	$0.32 \pm 0.05$
$19.0 \pm 0.2$	$0.38 \pm 0.06$
$20.3 \pm 0.2$	$0.90 \pm 0.15$
$21.6 \pm 0.2$	$1.63 \pm 0.26$
$22.1 \pm 0.2$	$1.21 \pm 0.20$
$23.8 \pm 0.2$	$2.39 \pm 0.39$
$24.3 \pm 0.2$	$2.32 \pm 0.38$
$24.8 \pm 0.2$	$2.60 \pm 0.42$
$26.5 \pm 0.2$	$3.45 \pm 0.56$
$26.5 \pm 0.2$	$2.97 \pm 0.48$
$29.0 \pm 0.2$	$3.32 \pm 0.54$
$31.9 \pm 0.2$	$2.94 \pm 0.48$
$35.3 \pm 0.2$	$2.39 \pm 0.39$

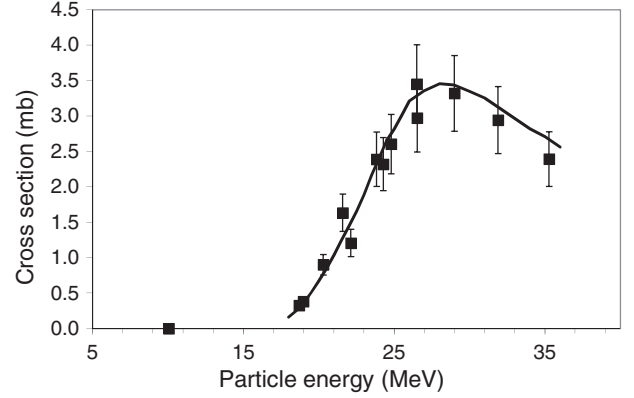


FIG. 3. Experimentally determined cross sections for the reaction  ${}^{230}\text{Th}({}^3\text{He},3n){}^{230}\text{U}$  (squares) in comparison with model calculations of neutron emission by using the EMPIRE-3 code (solid line).

sections on extended energy ranges beyond Kalbach Walker's parametrization.

The calculated cross sections associated with the relevant reaction mechanisms and the fission cross sections are presented in Fig. 2. The contribution of the statistical preequilibrium mechanism is negligible in the whole energy range of interest. The direct mechanism is the largest contributor to the reaction cross section, especially the nucleon transfer cross section dominated by the pickup mechanism ( ${}^3\text{He},\alpha$ ). The compound nucleus decay is fully dominated by the fission cross section in the whole energy range where the corresponding neutron emission is much lower.

#### IV. RESULTS AND DISCUSSION

The experimentally determined cross sections for the  ${}^{230}\text{Th}({}^3\text{He},3n){}^{230}\text{U}$  reaction are summarized in Table II and are shown in Fig. 3. This excitation function is measured here. The maximum of the  ${}^{230}\text{Th}({}^3\text{He},3n){}^{230}\text{U}$  excitation

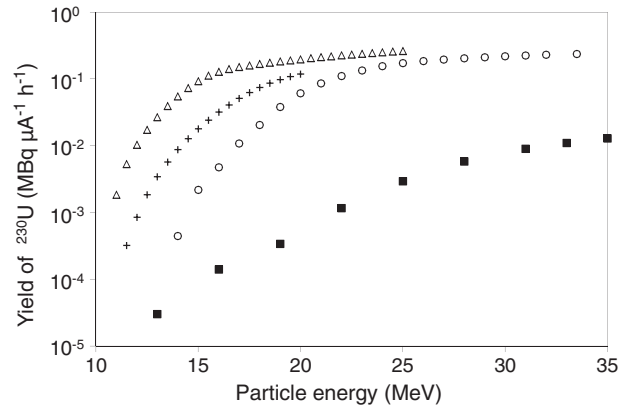


FIG. 4. Thick target yields of  ${}^{230}\text{U}$  produced *via* the  ${}^{230}\text{Th}({}^3\text{He},3n){}^{230}\text{U}$  reaction calculated from the experimental excitation function presented in this paper (squares). For comparison, literature data on the thick target yields of  ${}^{230}\text{U}$  produced *via* the reactions  ${}^{231}\text{Pa}(p,2n){}^{230}\text{U}$  (triangles),  ${}^{231}\text{Pa}(d,3n){}^{230}\text{U}$  (crosses), and  ${}^{232}\text{Th}(p,3n){}^{230}\text{Pa}(\beta^-){}^{230}\text{U}$  (28 days after end of bombardment, circles) are shown [2–4].

TABLE III. Comparison of the production routes for  $^{230}\text{U}$  and their yields.

Reaction	Maximum cross section (mb)	Thick target yield ( $\text{MBq } \mu\text{A}^{-1} \text{ h}^{-1}$ )	Reference
$^{230}\text{Th}(^3\text{He},3n)^{230}\text{U}$	$3.45 \pm 0.6$ (26.5 MeV)	0.013 (35 MeV)	This paper
$^{231}\text{Pa}(d,3n)^{230}\text{U}$	$27.8 \pm 3.4$ (17.9 MeV)	0.119 (20.0 $\rightarrow$ 11.0 MeV, oxide)	[4]
$^{231}\text{Pa}(p,2n)^{230}\text{U}$	$33.2 \pm 5.3$ (14.6 MeV)	0.245 (24.0 $\rightarrow$ 10.5 MeV, oxide)	[3]
$^{232}\text{Th}(p,3n)^{230}\text{Pa}(\beta^-)^{230}\text{U}$	$353 \pm 15$ (19.9 MeV)	$8.4^a$ (33.5 MeV)	[2]

<sup>a</sup>Thick target yield of  $^{230}\text{Pa}$ . The maximum activity of  $^{230}\text{U}$  is formed 4 weeks after the end of irradiation *via*  $\beta^-$  decay of  $^{230}\text{Pa}$  and corresponds to 2.82% of the activity of  $^{230}\text{Pa}$  initially produced. The available amount of  $^{230}\text{U}$  corresponds, thus, to a yield of  $0.24 \text{ MBq } \mu\text{A}^{-1} \text{ h}^{-1}$ .

function ( $3.45 \pm 0.56$  mb) was found at  $26.5 \pm 0.2$  MeV, which is very close to the theoretically estimated Coulomb barrier of 26 MeV. The measured and the calculated cross sections for the  $^{230}\text{Th}(^3\text{He},3n)^{230}\text{U}$  reaction are presented in Fig. 3. The agreement is surprisingly good when considering the assumptions and approximations explained in Sec. III. The theoretical calculations fully support the experimental data, however, we should bear in mind that uncertainties of the theoretical modeling are significant below 22 MeV, especially uncertainties of the employed Kalbach Walker's parametrization of the breakup and transfer cross sections.

Based on the cross sections experimentally determined in this paper, thick target yields for the production of  $^{230}\text{U}$  by  $^3\text{He}$  irradiation of  $^{230}\text{Th}$  were calculated (Fig. 4). The thick target yield was found to be  $0.013 \text{ MBq } \mu\text{A}^{-1} \text{ h}^{-1}$  at 35 MeV. As expected from the model calculations, the production yield of the reaction studied in this paper is too low for production purposes. Table III gives a summary of the nuclear reactions reported so far for the production of  $^{230}\text{U}$ . The processes, based on proton irradiation of  $^{232}\text{Th}$  or  $^{231}\text{Pa}$ , provide significantly higher yields and are more favorable for large-scale routine production.

- [1] A. Morgenstern, K. Abbas, F. Bruchertseifer, and C. Apostolidis, *Curr. Radiopharm.* **1**, 135 (2008).
- [2] A. Morgenstern, C. Apostolidis, F. Bruchertseifer, R. Capote, T. Gouder, F. Simonelli, M. Sin, and K. Abbas, *Appl. Radiat. Isot.* **66**, 1275 (2008).
- [3] A. Morgenstern, O. Lebeda, J. Stursa, F. Bruchertseifer, R. Capote, J. McGinley, G. Rasmussen, M. Sin, B. Zielinska, and C. Apostolidis, *Anal. Chem.* **80**, 8763 (2008).
- [4] A. Morgenstern, O. Lebeda, J. Stursa, R. Capote, M. Sin, F. Bruchertseifer, B. Zielinska, and C. Apostolidis, *Phys. Rev. C* **80**, 054612 (2009).
- [5] M. Avrigeanu, V. Avrigeanu, and A. J. Koning, *Phys. Rev. C* **85**, 034603 (2012).
- [6] M. Wallenius, A. Morgenstern, C. Apostolidis, and K. Mayer, *Anal. Bioanal. Chem.* **374**, 379 (2002).
- [7] N. A. Talvitie, *Anal. Chem.* **44**, 280 (1972).
- [8] J. F. Ziegler, J. P. Biersack, and U. Littmark, *SRIM 2003 Code. The Stopping and Range of Ions in Solids* (Pergamon, New York, 2003).
- [9] IAEA, Charged-Particle Cross Section Database for Medical Radioisotope Production, online at [http://www-nds.iaea.org/medical/monitor\\_reactions.html](http://www-nds.iaea.org/medical/monitor_reactions.html) (update March 2007).
- [10] R. B. Firestone, C. M. Baglin, and F. S. Y. Chu, *Table of Isotopes*, 8th ed. (Wiley, New York, 1998).
- [11] European Commission, Joint Research Centre, Institute for Transuranium Elements, Nucleonica – Web driven nuclear science, online at <http://www.nucleonica.net/index.aspx>.
- [12] S. Pommé, T. Altzitzoglou, R. Van Ammel, G. Suliman, M. Marouli, V. Jobbágy, J. Paepen, H. Stroh, C. Apostolidis, K. Abbas, and A. Morgenstern, *Appl. Radiat. Isot.* **70**, 1900 (2012).
- [13] S. Pommé, G. Suliman, M. Marouli, R. Van Ammel, V. Jobbágy, J. Paepen, H. Stroh, C. Apostolidis, K. Abbas, and A. Morgenstern, *Appl. Radiat. Isot.* **70**, 1913 (2012).
- [14] G. Suliman, S. Pommé, M. Marouli, R. Van Ammel, V. Jobbágy, J. Paepen, H. Stroh, C. Apostolidis, K. Abbas, and A. Morgenstern, *Appl. Radiat. Isot.* **70**, 1907 (2012).
- [15] M. Marouli, S. Pommé, J. Paepen, R. Van Ammel, V. Jobbágy, A. Dirican, G. Suliman, H. Stroh, C. Apostolidis, K. Abbas, and A. Morgenstern, *Appl. Radiat. Isot.* **70**, 2270 (2012).
- [16] M. Herman, P. Obložinský, R. Capote, M. Sin, A. Trkov, A. Ventura, and V. Zerkin, in *Proceeding of the International Conference on Nuclear Data for Science and Technology*, edited by R. C. Haight, M. B. Chadwick, T. Kawano, and P. Talou (AIP, New York, 2005) [*AIP Conf. Proc.* **769**, 1184, (2005)].
- [17] M. Herman, R. Capote, B. V. Carlson, P. Obložinský, M. Sin, A. Trkov, H. Wienke, and V. Zerkin, *Nucl. Data Sheets* **108**, 2655 (2007).
- [18] R. Capote, M. Sin, A. Trkov, M. Herman, B. V. Carlson, and P. Obložinský, in *International Conference on Nuclear Data for Science and Technology, Nice, France, 2007*, edited by O. Bersillon, F. Gunsing, E. Bauge, R. Jacqmin, and S. Leray (EDP Sciences, Les Ulis, France, 2008), p. 255. Available online at <http://dx.doi.org/10.1051/ndata:07755>.

- [19] J. Raynal, in *Computing as a Language of Physics. ICTP International Seminar Course at Trieste from 2 to 20 Aug. 1971* (IAEA, Vienna, 1972), p. 281.
- [20] C. Kalbach Walker, report to the 2nd RCM of the FENDL-3 CRP, 2010 (unpublished). Available online at <http://www-nds.iaea.org/fendl3/docs/dBreakupRCM2.pdf>
- [21] C. Kalbach Walker, PRECO 2006: Exciton Model Preequilibrium Nuclear Reaction Code with Direct Reactions (BNL, Upton, New York, 2007). Available online at <http://www.nndc.bnl.gov/nndcscr/model-codes/preco-2006/>
- [22] M. Sin, R. Capote, A. Ventura, M. Herman, and P. Obložinský, *Phys. Rev. C* **74**, 014608 (2006).
- [23] M. Sin and R. Capote, *Phys. Rev. C* **77**, 054601 (2008).
- [24] M. Sin, P. Obložinský, M. Herman, and R. Capote, *J. Korean Phys. Soc.* **59**, 1015 (2011).
- [25] R. Capote *et al.*, *Nucl. Data Sheets* **110**, 3107 (2009).
- [26] F. D. Becchetti, Jr. and G. W. Greenlees, Annual technical report of the J. H. Williams Laboratory, University of Minnesota, 1969 (unpublished).
- [27] R. Capote, E. S. Soukhovitskii, J. M. Quesada, and S. Chiba, *Phys. Rev. C* **72**, 064610 (2005).
- [28] R. Capote, E. S. Soukhovitskii, J. M. Quesada, and S. Chiba, in *International Conference on Nuclear Data for Science and Technology, Nice, France, 2007*, edited by O. Bersillon, F. Gunsing, E. Bauge, R. Jacqmin, and S. Leray (EDP Sciences, Les Ulis, France, 2008). Available online at <http://dx.doi.org/10.1051/ndata:07765>
- [29] S. Goriely, S. Hilaire, and A. J. Koning, *Phys. Rev. C* **78**, 064307 (2008).